The DIGILATOR, a New Broadband Microwave Frequency Translator

GERALD KLEIN, SENIOR MEMBER, IEEE, AND LEONARD DUBROWSKY, MEMBER, IEEE

Abstract—**Frequency translation of an RF wave can be accomplished by subjecting it to a constant rate of phase shift or by applying an ideal repetitive sawtooth phase function which snaps to zero at 360 degrees (serrodyne modulation). The DIGILATOR is a new type of frequency translator which employs a multibit latching ferrite phase shifter with a suitable digital switching driver to obtain a multiple-step approximation to the serrodyne phase function.**

This paper reviews the theory of an *N*-step DIGILATOR and describes the design of a 16-step, *X*-band device. Experiments showed that performance is independent of microwave frequency over the design frequency band of the phase shifter. The carrier and close-in sidebands were suppressed by 39 dB and predicted far-out sidebands were within 1 dB of theoretical amplitudes.

I. Introduction

FREQUENCY translation of an ac wave is the changing of frequency without the generation of significant energy at unwanted output frequencies. This definition differentiates the frequency translator from the usual single sideband modulator in which a number of strong signals at new frequencies are generated, and the desired signal is selected by filtering. Frequency translators operate on the principle that when an ac wave of form

$$e_0 = \sin (2\pi f_0 t + \theta)$$

is subjected to a θ which varies linearly with time such as

$$\theta = kt = (2\pi f_m)t$$

the resultant is

$$e_0 = \sin (2\pi f_0 t + 2\pi f_m t) = \sin 2\pi (f_0 + f_m)t.$$

This is ideal frequency translation to a new frequency (f_0+f_m). This frequency shift is similar to the familiar Doppler frequency shift caused by the reflections of a wave from a moving object. A constant Doppler frequency shift is produced by a constant rate of change in electrical phase length between the source and the reflector. Figure 1 shows how ideal frequency translation can also be accomplished by employing a repetitive sawtooth phase function which repeats after a phase traversal of 360 degrees. The name "serrodyne" has been employed to describe this form of phase modulation.

Jaffe [1] discussed the limitations of many of the methods previously used for linear and serrodyne phase modulation for frequency translation. These include the mechanical rotating continuous linear phase shifter [2], the ferrite equivalent of the mechanical phase shifter [3], the ferrite serrodyne modulator [4], the traveling wave tube serrodyne modulator [5], and the semiconductor serrodyne modulator [6]. He described an extension of the method presented by Rutz [7] employing diode switching to obtain a stepped approximation to serrodyne modulation. Both Jaffe and Rutz were limited to a three-step approximation by high losses associated with the diode switches. Total conversion losses in the order of 4 to 6 dB were observed, and operation was narrowband with relatively poor suppression of unwanted sidebands.

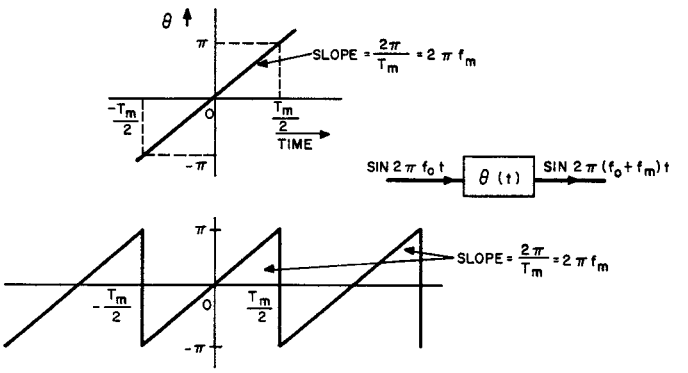

Fig. 1. Phase functions for ideal frequency translation.

The DIGILATOR is a new device for accomplishing small frequency translations in the microwave range which overcomes some of the disadvantages of previous techniques. It employs the latching ferrite phase shifter [8], [9] and a digital switching driver to obtain a multiple-step approximation to the sawtooth phase function. Since the number of steps employed to achieve 360-degree differential phase shift does not greatly affect the insertion loss of a latching phase shifter, an 8-, 16-, or 32-step approximation can readily be achieved with low conversion loss and good suppression of unwanted sidebands.

II. The Digital Ferrite Phase Shifter

Figure 2 shows the basic geometry of a digital phase shifter element and its associated magnetization curve. Through its single turn coil, a current pulse lasting a fraction of a microsecond is employed to obtain a magnetization beyond the point at which the hysteresis loop closes. When the current falls to zero, the flux in the core returns to its high remanent state.

Manuscript received July 5, 1966; revised October 21, 1966.

The authors are with the Westinghouse Defense and Space Center, Aerospace Division, Baltimore, Md.

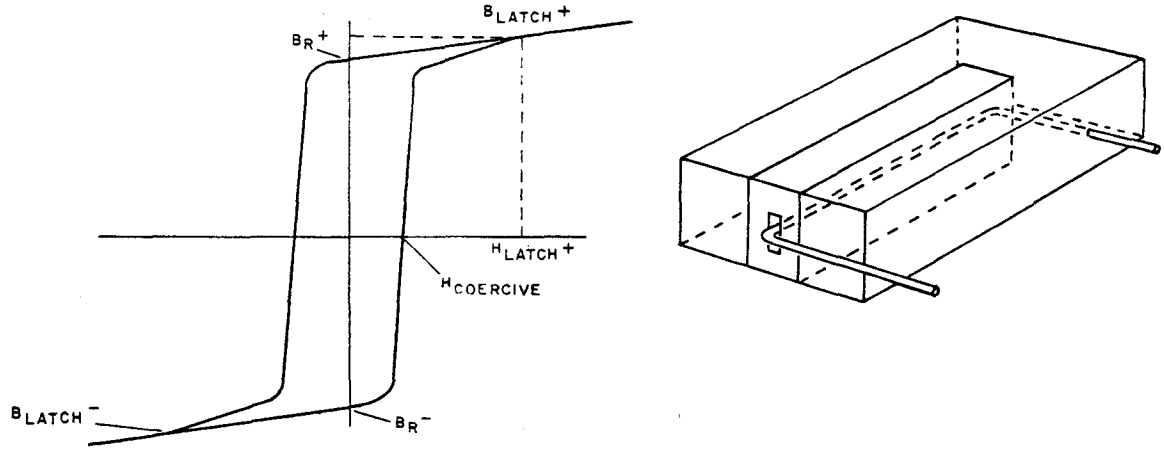

Fig. 2. Basic geometry of digital phase-shifter element and its hysteresis loop.

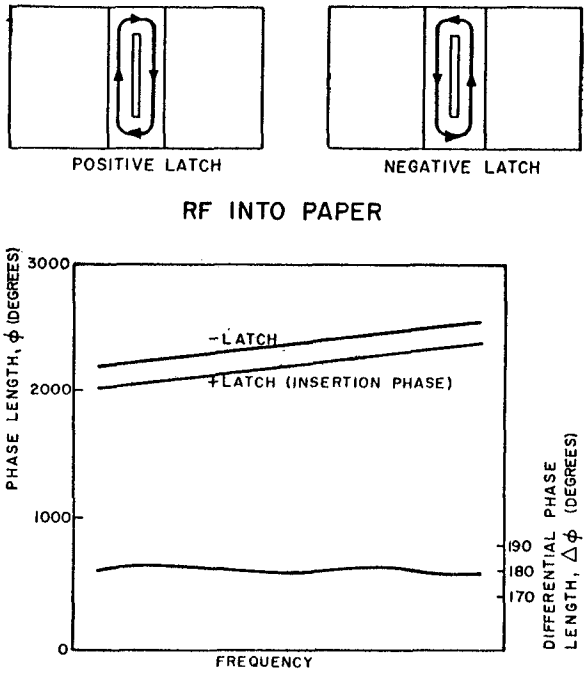

Fig. 3. Remanent magnetization states and resulting phase versus frequency.

A reverse polarity current pulse can later be applied to saturate the material in the opposite direction, switching the flux to the opposite remanent state. Since the magnetic circuit is continuous through the ferrite, there is virtually no leakage field, and the switching energy is low. Figure 3 shows the effect of the two remanent magnetization states on the electrical length of the ferrite loaded waveguide. It is seen that differential phase shift is caused by a perturbation in the propagation constant on the order of 10 percent. By proper adjustment of toroid geometry, it is possible to establish conditions for $\Delta\phi$ constant to ± 1 percent over a 10-percent frequency band. Since a particular value of $\Delta\phi$ is obtained with a given length bit, a series of different length bits providing $\Delta\phi$ of 180, 90, 45 degrees, etc., can be cascaded in a straight waveguide section to provide digital steps from 0 to 360 degrees.

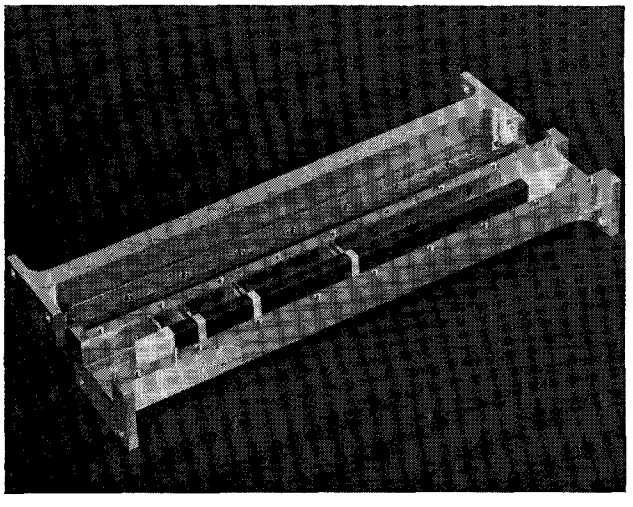

Fig. 4. X-band, 4-bit digital ferrite phase shifter.

X-band 3- to 5-bit digital phase shifters have been developed [10] with switching speeds under 1 μs and switching energy less than 1 μJ/deg of RF phase change. These devices can operate over a 10- to 30-percent bandwidth with peak power capabilities up to 50 kW at an average power up to 500 watts. Insertion loss of these phase shifters is under 1.0 dB. Figure 4 shows a typical 4-bit X-band ferrite phase shifter with the top waveguide wall removed. The dielectric spacers between the bits are used to prevent magnetic interaction.

III. The DIGILATOR

A. Basic Concepts

The availability of a low loss, broadband, fast switching microwave phase shifter makes it of interest to consider the properties of a multiple-step approximation to ideal serrodyne phase modulation.

When an ideal multistep approximation such as that shown in Fig. 5 is analyzed (see Appendix) it is found that the input frequency and all undesired harmonics of f_m are

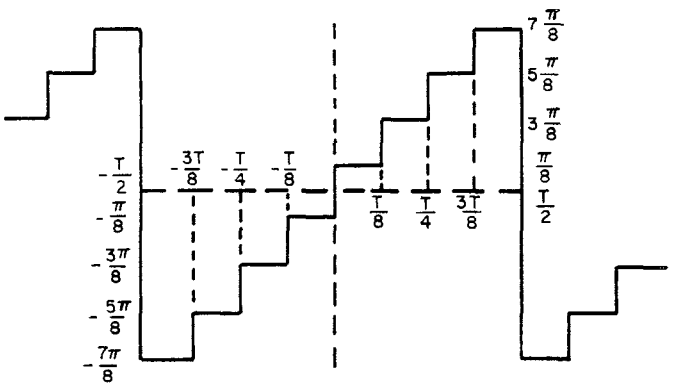

Fig. 5. Eight-step approximation to ideal serrodyne function.

TABLE I
SPECTRAL AMPLITUDES FOR VARIOUS VALUES OF N

N	4	8	16	32.
Spectral line	Spectral amplitude-dB relative to 1st harmonic			
f_0+1f_m (Reference for remaining frequencies)	0.91*	0.22*	0.05*	0*
−3	9.5	—	—	—
+5	14.0	—	—	—
−7	16.9	16.9	—	—
+9	19.1	19.1	—	—
−11	20.8	—	—	—
+13	22.3	—	—	—
−15	23.5	23.5	23.5	—
+17	24.6	24.6	24.6	—
−19	25.6	—	—	—
+21	26.4	—	—	—
−23	27.2	27.2	—	—
+25	28.0	28.0	—	—
−27	28.6	—	—	—
+29	29.2	—	—	—
−31	29.8	29.8	29.8	29.8
+33	30.4	30.4	30.4	30.4

* Relative to carrier.

infinitely suppressed with the exception of those at frequencies given by

$$f_{out} = f_0 + (kN + 1)f_m \quad \text{upper sidebands}$$

and

$$f_{out} = f_0 - (kN - 1)f_m \quad \text{lower sidebands}$$

where N is the number of steps employed in the approximation, and k assumes all integer values from zero to infinity for the upper sidebands and unity to infinity for the lower sidebands.

The amplitudes of the predicted output frequencies for a lossless microwave circuit are given by

$$|e_0| = \frac{E}{(kN \pm 1)} \frac{\sin \pi/N}{\pi/N} \simeq \frac{E}{(kN \pm 1)}.$$

The spectral amplitudes for $N=4$, 8, 16, and 32 are listed in Table I.

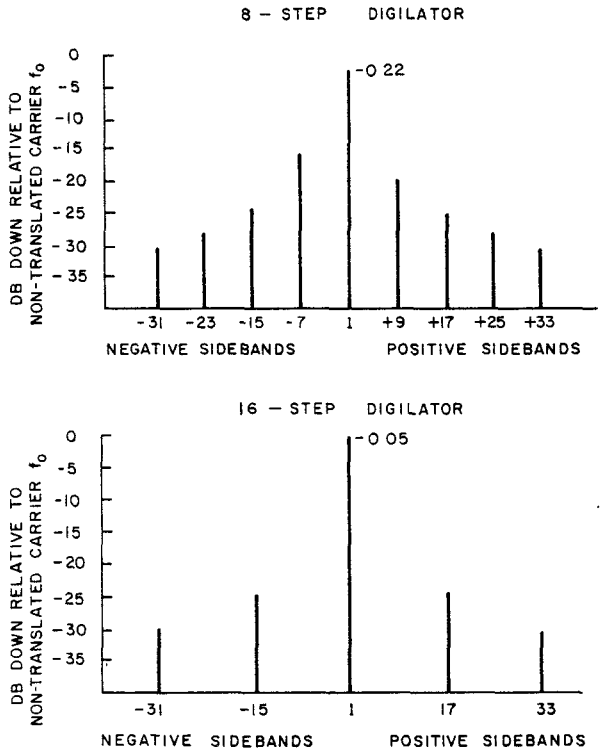

Fig. 6. Spectra of ideal 8- and 16-step DIGILATORS.

Figure 6 shows the theoretical output spectra of an 8- and a 16-step DIGILATOR. It is seen that the amplitudes of the predicted outputs at each frequency varies inversely with the frequency distance from the input signal, and that the effect of increasing N is to increase the spacing between predicted outputs by suppressing certain frequencies without affecting the amplitude of the remaining signals. By combining the expressions for output frequencies and amplitudes we see that for the upper sidebands:

$$|e|_{out} \propto \left|\frac{1}{kN+1}\right| = \left|\frac{1}{\frac{f_{out}-f_0}{f_m}}\right| = \left|\frac{1}{\frac{nf_m}{f_m}}\right| = \frac{1}{n}$$

where n is the frequency distance from f_0 of each component in multiples of f_m. A similar result can be obtained for the lower sidebands.

B. Effects of Phase Errors

A computer analysis was performed to determine the effects of individual step phase errors in the order of a few degrees. Phase tolerances of this magnitude can readily be maintained in devices.

Table II shows the computed spectral amplitudes for an 8-step, 3-bit DIGILATOR and a 16-step, 4-bit DIGILATOR for 0, 1, and 2 degrees error per bit. It is interesting to note that the predicted sidebands for the ideal case maintain a constant amplitude even though the phase error per bit varies. In addition, it appears that there is complete suppression of those spectral lines which are integral multiples of the number of phase steps used as indicated by the > -70 dB computed values.

TABLE II

EFFECTS OF PHASE ERRORS ON COMPUTED AMPLITUDE OF SPECTRAL LINES (dB) FOR 8- AND 16-STEP DIGILATOR

Spectral* line number	8-step			16-step		
	Phase error per bit			Phase error per bit		
	0°	1°	2°	0°	1°	2°
0	$-\infty$	−45.5	−39.3	$-\infty$	−45.7	−39.5
+1	−0.22	−0.22	−0.22	−0.05	−0.05	−0.07
±2	$-\infty$	−46.0	−39.9	$-\infty$	−45.8	−39.3
±3	$-\infty$	−43.4	−37.3	$-\infty$	−44.9	−38.9
±4	$-\infty$	−56.0	−50.4	$-\infty$	−55.4	−48.9
±5	$-\infty$	−47.8	−41.7	$-\infty$	−45.7	−39.5
±6	$-\infty$	−53.9	−48.4	$-\infty$	−60.1	−53.9
−7	−17.1	−17.1	−17.1	$-\infty$	−44.1	−38.1
±8	$-\infty$	> −70.8	> −70.7	$-\infty$	−62.5	−56.3
+9	−19.3	−19.3	−19.3	$-\infty$	−46.3	−40.3
±10	$-\infty$	−62.5	−54.9	$-\infty$	−63.7	−57.9
±11	$-\infty$	−54.6	−48.6	$-\infty$	−52.2	−46.2
±12	$-\infty$	−65.1	−59.4	$-\infty$	−63.2	−57.6
±13	$-\infty$	−56.0	−50.0	$-\infty$	−57.0	−51.4
±14	$-\infty$	−59.7	−54.9	$-\infty$	−59.1	−54.3
−15	−23.8	−23.8	−23.8	−23.6	−23.5	−23.6
±16	$-\infty$	> −70.7	> −70.7	$-\infty$	> −70.3	> −70.7
+17	−24.8	−24.8	−24.9	−24.6	−24.7	−24.7
±18	$-\infty$	−71.0	−61.3	$-\infty$	−70.5<	−60.7
±19	$-\infty$	−59.4	−53.4	$-\infty$	−61.5	−55.2
±20	$-\infty$	−69.0	−63.6	$-\infty$	−71.6	−64.0
±21	$-\infty$	−60.2	−54.2	$-\infty$	−58.5	−52.2
±22	$-\infty$	−62.3	−58.0	$-\infty$	−72.4<	−65.6
−23	−27.5	−27.5	−27.5	$-\infty$	−54.5	−48.5
±24	$-\infty$	> −70.7	> −70.7	$-\infty$	−71.7<	−65.6
+25	−28.2	−28.2	−28.2	$-\infty$	−55.2	−49.2
±26	$-\infty$	−79.7	−65.9	$-\infty$	−71.2<	−65.9
±27	$-\infty$	−62.5	−56.4	$-\infty$	−59.7	−53.9
±28	$-\infty$	−71.6	−66.3	$-\infty$	−69.1	−64.1
±29	$-\infty$	−63.0	−57.0	$-\infty$	−62.9	−57.8
±30	$-\infty$	−63.9	−60.0	$-\infty$	−63.3	−59.4
−31	−30.0	−30.0	−30.0	−29.9	−29.9	−29.7
±32	$-\infty$	> −70.7	> −70.7	$-\infty$	> −70.3	> −70.3
+33	−30.6	−30.6	−30.6	−30.4	−30.4	−30.5

* Stronger of two signals. Amplitudes relative to input signal at f_0.

C. Driver Circuits

In order to form the step phase function with a 4-bit phase shifter, the bits must be switched in the sequence shown in Table III. This produces a 16-step phase function.

The $22\frac{1}{2}$-degree bit must switch at a rate of $16f_m$, the 45-degree bit at $8f_m$, the 90-degree bit at f_m, and the 180-degree bit at $2f_m$. A simplified diagram of the circuits employed for the switching is shown in Fig. 7. The oscillator is run at 16 times the desired translation frequency and is divided down by integrated circuits to provide the proper switching sequence to the SCR drivers.

D. Limitations

The energy per unit volume required to switch a digital ferrite phase shifter is a constant for a particular material. Therefore, although the total energy required to switch a short bit is smaller than that for a long bit, the energy density is constant and the dissipated power density and resulting temperature rise is proportional to the switching rate. When employing digital logic of the form of Table III to generate a step phase function, the upper limits on translation frequency set both by ferrite heating and driver switching speed will be determined by requirements of the smallest bit, which is switched at a rate of 2^B times the translation frequency for a phase shifter with B bits.

An X-band phase shifter can typically be switched in 1 μs or slower, with an energy in the order of 1 μJ/deg of phase shift. As switching time decreases below 0.8 μs, switching energy rises rapidly. For a 16-step, 4-bit DIGILATOR translating at a 62.5-kHz rate (smallest bit switching at 1 MHz), the total ferrite power dissipation would be about 90 watts.

Some form of cooling would be required to stabilize the ferrite temperature under these conditions. State-of-the-art SCR drivers can be designed to switch at a 320-kHz rate, limiting the upper translation frequency for a 4-bit DIGILATOR to 20 kHz. Since a driver efficiency in the order of 50 percent can be achieved, overall input power for 20-kHz translation would be about 60 watts. Present research on miniature ferrite phase shifters and transistor drivers is directed toward raising this upper translation frequency to 1 MHz.

The magnetization of ferrite materials is known to be temperature sensitive. An X-band, 180-degree phase shifter em-

ploying a temperature-stabilized garnet material exhibits a variation in phase of 0.4 degree per degree centigrade change in ambient. To achieve accurate phase control, it is necessary either to stabilize ambient temperature or to provide a drive circuit which varies the applied latching current pulses to compensate for temperature change. Such techniques are feasible for latching ferrite phase shifters.

E. Experimental Results

The DIGILATOR was implemented by using a 4-bit ferrite phase shifter in a WR90 waveguide, similar to that shown in Fig. 4, to provide the desired π, $\pi/2$, $\pi/4$, and $\pi/8$ changes in electrical length. The material used was Trans Tech G1001. The cross section of the toroid was 0.180 inch by 0.400 inch with a central slot of 0.020 inch by 0.240 inch. It has been determined that this cross section provides a 1-percent differential phase deviation over an 8.5- to 9.5-GHz band. The length of the π bit was 3.176 inches, the smaller bits being proportionately shorter. The microwave structure

TABLE III
DIGITAL LOGIC FOR 16-STEP DIGILATOR

Relative phase	Bit latch states			
	22½°	45°	90°	180°
0	+	+	+	+
22½	−	+	+	+
45	+	−	+	+
67½	−	−	+	+
90	+	+	−	+
112½	−	+	−	+
135	+	−	−	+
157½	−	−	−	+
180	+	+	+	−
202½	−	+	+	−
225	+	−	+	−
247½	−	−	+	−
270	+	+	−	−
292½	−	+	−	−
315	+	−	−	−
337½	−	−	−	−
0	+	+	+	+

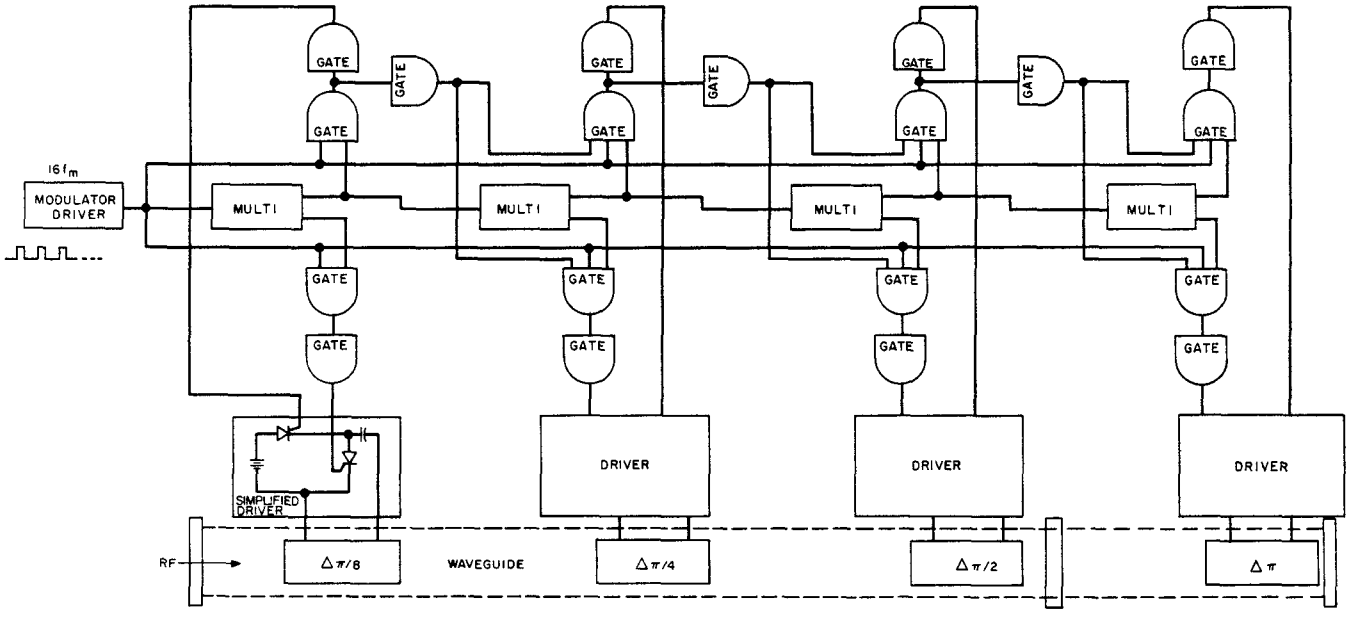

Fig. 7. DIGILATOR driver circuits.

is matched using two-step dielectric impedance transformers, yielding a VSWR of under 1.15 to 1 over the band.

Dielectric spacers ($\epsilon = 15$) of the same toroidal configuration were placed between the bits to prevent magnetic interaction. The nominal insertion loss of the device was 0.8 dB.

The driver furnished a 15-ampere pulse at 65 volts in order to perform the switching operations in 1.5 μs. A translation frequency of 30 Hz was employed in the experimental device.

Table IV shows the results of measurements made on the *X*-band, 16-step DIGILATOR over the frequency range of 8.5 to 9.5 GHz. It is seen that performance is essentially independent of microwave frequency and that suppression of all unexpected sidebands was greater than 39 dB. The largest phase error in the 4 bits employed for this test was 2 degrees. Thus, the measured carrier suppression compares well with the computer predicted value.

TABLE IV
16-STEP DIGILATOR

Spectral line	Predicted (dB)	Measured (dB)*		
		8.5 GHz	9.1 GHz	9.5 GHz
0	$-\infty$	—	−39	—
+1	reference	—	reference	—
−15	−23.6	−24.3	−24.5	−23.2
+17	−24.6	−24.0	−24.5	−24.3
−31	−29.9	−29.3	−29.7	−29.5
+33	−30.4	−29.7	−30.2	−30.0

* All unlisted lines > − 40 dB down.

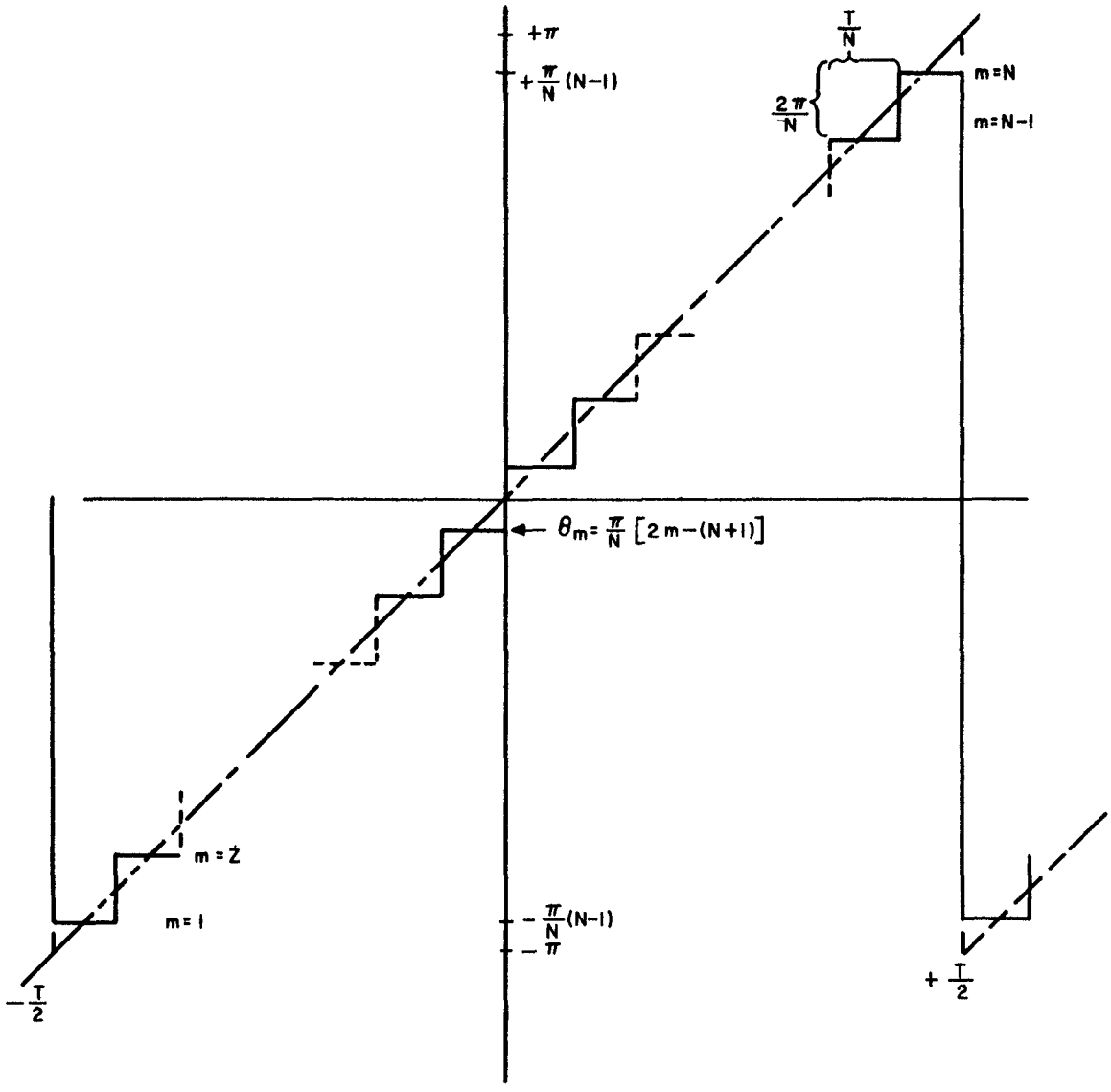

Fig. 8. Phase function of the ideal N-step DIGILATOR.

IV. Conclusion

A new form of ferrite frequency translator, the DIGILATOR, has been developed for which experimental performance has shown excellent agreement with theoretical predictions.

Development of digital ferrite phase shifters has resulted in C-band, 360-degree units with under 0.5-dB loss and X-band devices with under 0.8-dB loss capable of operating at hundreds of watts of average power over a 10-percent frequency band with constant $\Delta\theta$. Thus, the DIGILATOR can be applied as a broadband high-level modulator directly at the output of a transmitter. This device offers many new possibilities for lowloss broadband microwave signal processing.

Appendix

DIGILATOR Spectrum Analysis

The output waveform of the DIGILATOR can be expressed as:

$$e_0 = g(t) \sin [\omega_0 t + \theta(t)] \tag{1}$$

where

ω_0 = microwave carrier radian frequency.
$\theta(t)$ = the periodic phase modulation.
$g(t)$ = signal amplitude. For the ferrite digital phase shifter the loss is nearly independent of phase. Therefore, $g(t)$ can be replaced by a constant E.

Expanding (1) we obtain

$$e_0 = E[\cos \theta(t) \sin \omega_0 t + \sin \theta(t) \cos \omega_0 t]. \tag{2}$$

Figure 8 shows the $\theta(t)$ waveform for an N-step DIGILATOR.

Representing the functions $\cos \theta(t)$ and $\sin \theta(t)$ (periodic over the interval T, or $\omega = 2\pi/T$) by Fourier series

$$\sin \theta(t) = \frac{A_0}{2} + \sum_{n=1}^{\infty} (a_n \cos n\omega t + b_n \sin n\omega t) \tag{3}$$

$$\cos\theta(t) = \frac{C_0}{2} + \sum_{n=1}^{\infty} (c_n \cos n\omega t + d_n \sin n\omega t) \quad (4)$$

where

$$A_0 = \frac{2}{T}\int_{-T/2}^{+T/2} \sin\theta(t)dt \quad (5)$$

$$C_0 = \frac{2}{T}\int_{-T/2}^{+T/2} \cos\theta(t)dt \quad (6)$$

$$a_n = \frac{2}{T}\int_{-T/2}^{+T/2} \sin\theta(t)\cos n\omega t dt \quad (7)$$

$$b_n = \frac{2}{T}\int_{-T/2}^{+T/2} \sin\theta(t)\sin n\omega t dt \quad (8)$$

$$c_n = \frac{2}{T}\int_{-T/2}^{+T/2} \cos\theta(t)\cos n\omega t dt \quad (9)$$

$$d_n = \frac{2}{T}\int_{-T/2}^{+T/2} \cos\theta(t)\sin n\omega t dt. \quad (10)$$

For the ideal DIGILATOR we see that $\theta(t)$ is always an odd function and $\Delta\theta = 2\pi$ for $\Delta t = T$. Therefore,

$$A_0 = C_0 = a_n = d_n = 0.$$

This reduces (3) and (4) to

$$\sin\theta(t) = \sum_{n=1}^{\infty} b_n \sin n\omega t \quad (11)$$

$$\cos\theta(t) = \sum_{n=1}^{\infty} c_n \cos n\omega t. \quad (12)$$

Inserting (11) and (12) into (2) and combining terms we obtain

$$e_0 = \frac{E}{2}\sum_{n=1}^{\infty}[(c_n + b_n)\sin(\omega_0 + n\omega)t + (c_n - b_n)\sin(\omega_0 - n\omega)t]. \quad (13)$$

The carrier is completely suppressed. The amplitudes of the upper sidebands at frequencies $(\omega_0+n\omega)$ are given by $E/2(c_n+b_n)$ and the lower sidebands at frequencies $(\omega_0-n\omega)$ are given by $E/2(c_n-b_n)$. Referring to Fig. 8, when the phase function is divided into N-steps, each phase step is equal to $2\pi/N$ in magnitude and the total excursion of the function is $2\pi/N(N-1)$ as time varies between $-T/2$ and $+T/2$ in steps of T/N. If we establish $\theta=0$ at $T=0$ as a reference, the function is odd and varies over the range

$$-\frac{\pi}{N}(N-1) \le \theta \le +\frac{\pi}{N}(N-1).$$

For the mth step

$$\theta_m = -\frac{\pi}{N}(N-1) + (m-1)\frac{2\pi}{N} = \frac{\pi}{N}[2m - (N+1)] \quad (14)$$

and

$$-\frac{T}{2} + (m-1)\frac{T}{N} \le t_n \le -\frac{T}{2} + m\frac{T}{N}$$

or

$$\frac{T}{N}\left[(m-1) - \frac{N}{2}\right] \le t_n \le \frac{T}{N}\left[m - \frac{N}{2}\right]. \quad (15)$$

Inserting (14) and (15) into (8) and (9), the expression for b_n and c_n, we obtain

$$b_n = \frac{2}{T}\sum_{m=1}^{N}\int_{T/N[(m-1)-N/2]}^{T/N(m-N/2)} \sin\frac{\pi}{N}[2m - (N+1)] \cdot \sin n\omega t dt \quad (16)$$

$$c_n = \frac{2}{T}\sum_{m=1}^{N}\int_{T/N[(m-1)-N/2]}^{T/N(m-N/2)} \cos\frac{\pi}{N}[2m - (N+1)] \cdot \cos n\omega t dt. \quad (17)$$

Evaluating the integrals of (16) and (17) and recognizing that $\omega T = 2\pi$ and $\sin[x+(n-1)\pi] = (-1)^{n+1}\sin x$, we find that

$$e_0^+ = \frac{E}{2}(c_n + b_n) = \frac{E(-1)^{n+1}}{n2\pi}\sum_{m=1}^{N}\sin\frac{\pi}{N}[2m(n-1)+1] - \sin\frac{\pi}{N}[2m(n-1) - 2n + 1] \quad (18)$$

$$e_0^- = \frac{E}{2}(c_n - b_n) = \frac{E(-1)^{n+1}}{n2\pi}\sum_{m=1}^{N}\sin\frac{\pi}{N}[2m(n+1)-1] - \sin\frac{\pi}{N}[2m(n+1) - 2n - 1]. \quad (19)$$

Breaking down the sine functions to separate terms containing m

$$e_0^+ = \frac{E(-1)^{n+1}}{n2\pi}\left\{\left[\cos\frac{\pi}{N} - \cos\frac{\pi}{N}(1-2n)\right]\sum_{m=1}^{N} \cdot \sin\frac{2\pi m}{N}(n-1) + \left[\sin\frac{\pi}{N} - \sin\frac{\pi}{N}(1-2n)\right] \cdot \sum_{m=1}^{N}\cos\frac{2\pi m}{N}(n-1)\right\} \quad (20)$$

$$e_0^- = \frac{E(-1)^{n+1}}{n2\pi}\left\{\left[\cos\frac{\pi}{N} - \cos\frac{\pi}{N}(1+2n)\right]\sum_{m=1}^{N} \cdot \sin\frac{2\pi m}{N}(n+1) - \left[\sin\frac{\pi}{N} - \sin\frac{\pi}{N}(1+2n)\right] \cdot \sum_{m=1}^{N}\cos\frac{2\pi m}{N}(n+1)\right\}. \quad (21)$$

Using the equations for the sum of a trigonometric series [12]

$$\cos x + \cos 2x + \cdots + \cos Nx = \frac{\sin (2N+1)x/2}{2\sin\frac{x}{2}} - \frac{1}{2} \tag{22}$$

$$\sin x + \sin 2x + \cdots + \sin Nx = \frac{1}{2}\cot\frac{x}{2} - \frac{\cos (2N+1)x/2}{2\sin\frac{x}{2}}. \tag{23}$$

For our case, $x=2\pi/N(n-1)$ for e_0^+ and $x=2\pi/N(n+1)$ for e_0^-.

From (23) we find

$$\sum_{m=1}^{N} \sin\frac{2\pi m}{N}(n-1) = \sum_{m=1}^{N} \sin\frac{2\pi m}{N}(n+1) = 0$$

for all integer values of n. Therefore, (20) and (21) reduce to

$$e_0^+ = \frac{E(-1)^{n+1}}{n2\pi}\left[\sin\frac{\pi}{N} - \sin\frac{\pi}{N}(1-2n)\right]\sum_{m=1}^{N} \cdot\cos\frac{2\pi m}{N}(n-1) \tag{24}$$

$$e_0^- = \frac{E(-1)^{n+1}}{n2\pi}\left[\sin\frac{\pi}{N}(1+2n) - \sin\frac{\pi}{N}\right]\sum_{m=1}^{N} \cdot\cos\frac{2\pi m}{N}(n+1). \tag{25}$$

For e_0^+ we find from (22) that

$$\sum_{m=1}^{N} \cos\frac{2\pi m}{N}(n-1) = \frac{\sin\frac{\pi}{N}(n-1)}{2\sin\frac{\pi}{N}(n-1)} - \frac{1}{2} \tag{26}$$

if $(n-1)/N \neq k$ (k is any positive integer from 0 to $+\infty$) then from (26) we see that $e_0^+=0$. If $(n-1)/N=k$, $n=(kN+1)$, and from (24) we find

$$e_0^+ = \frac{E(-1)^{kN+2}}{2\pi(kN+1)}\left[2\sin\frac{\pi}{N}\right]N \tag{27}$$

or

$$|e_0^+| = \frac{E}{(kN+1)}\,\frac{\sin\frac{\pi}{N}}{\frac{\pi}{N}}. \tag{28}$$

These spectral lines appear at frequencies

$$f_{\text{out}} = f_0 + (kN+1)f\Big]_{k=0}^{k=+\infty}; \tag{29}$$

for e_0^- we find from (22) that

$$\sum_{m=1}^{N} \cos\frac{2\pi m}{N}(n+1) = \frac{\sin\frac{\pi}{N}(n+1)}{2\sin\frac{\pi}{N}(n+1)} - \frac{1}{2} \tag{30}$$

if $(n+1)/N \neq k$ (where k ranges from $+1$ to $+\infty$, since n cannot take on negative values), then from (30) we see that $e_0^-=0$. For $(n+1)/N=k$, $n=(kN-1)$, and from (25) we find

$$e_0^- = \frac{E(-1)^{kN}}{2\pi(kN-1)}\left[-2\sin\frac{\pi}{N}\right]N \tag{31}$$

or

$$|e_0^-| = \frac{E}{(kN-1)}\,\frac{\sin\frac{\pi}{N}}{\frac{\pi}{N}}. \tag{32}$$

These spectral lines appear at frequencies

$$f_{\text{out}} = f_0 - (kN-1)f\Big]_{k=+1}^{k=+\infty}. \tag{33}$$

Acknowledgment

The authors wish to acknowledge the assistance given them in the design of the drivers and logic circuitry by W. V. Hoff and M. G. Woolfson. Acknowledgment is also given to C. L. Fogle and R. E. Huber for the electronics and microwave implementation.

References

[1] J. S. Jaffe and R. C. Mackey, "Microwave frequency translator," *IEEE Trans. on Microwave Theory and Techniques*, vol. MTT-13, pp. 371–378, May 1965.
[2] A. G. Fox, "An adjustable waveguide phase changer," *Proc. IRE*, vol. 35, pp. 1489–1498, December 1947.
[3] J. Caheris, "Microwave single-sideband modulator using ferrites," *Proc. IRE*, vol. 42, pp. 1242–1247, August 1954.
[4] R. F. Soohoo, "Ferrite microwave phase shifters," *IRE Conv. Rec.*, pt. 5, pp. 84–98, 1956.
[5] R. C. Cummings, "The serrodyne frequency translator," *Proc. IRE*, vol. 45, pp. 175–186, February 1957.
[6] R. Hardin et al., "Electronically-variable phase shifters utilizing variable capacitance diodes," *Proc. IRE (Correspondence)*, pp. 944–945, May 1960.
[7] E. M. Rutz and J. E. Dye, "Frequency translation by phase modulation," *IRE WESCON Conv. Rec.*, pt. 1, pp. 201–207, 1957.
[8] M. A. Truehaft and L. M. Silber, "Use of microwave ferrite toroids to eliminate external magnets and reduce switching power," Polytechnic Institute of Brooklyn, N. Y., MRI Memo. 7, June 16, 1958.
[9] J. Woermbke and J. Myers, "Latching ferrite microwave devices," *Microwaves*, October 1964.
[10] L. Dubrowsky, G. Kern, and G. Klein, "A high power X-band latching digital ferrite phase shifter for phased array application," presented at the IEEE NEREM Conv., November 1965, Westinghouse Defense and Space Center Rept. DSC-5956, January 5, 1966.
[11] W. J. Ince and E. Stern, "Waveguide non-reciprocal remanence phase shifters," *Proc. Int. Conf. on Microwave Behavior of Ferromagnetics and Plasmas*, IEE, London, England, September 1965.
[12] E. A. Guilleman, *The Mathematics of Circuit Analysis*. New York: Wiley, 1949, p. 437.